EurJIC European Journal of Inorganic Chemistry

FULL PAPER

DOI: 10.1002/ejic.201200450

# A Phenylbenzothiazole Conjugate with the Tricarbonyl *fac*-$[M(I)(CO)_3]^+$ (M = Re, $^{99}$Tc, $^{99m}$Tc) Core for Imaging of β-Amyloid Plaques

**Marina Sagnou,[a] Stamatia Tzanopoulou,[a] Catherine P. Raptopoulou,[b] Vassilis Psycharis,[b] Henrik Braband,[c] Roger Alberto,[c] Ioannis C. Pirmettis,[d] Minas Papadopoulos,[d] and Maria Pelecanou*[a]**

**Keywords:** Medicinal chemistry / Imaging agents / Rhenium / Technetium / Alzheimer's disease

The 2-(4′-aminophenyl)-6-methylbenzothiazole that is known to display affinity and specificity toward the amyloid plaques of Alzheimer's disease (AD) has been joined to the tricarbonyl $[M(CO)_3NNO]$ chelate (M = Re, $^{99}$Tc, and $^{99m}$Tc) through a five-carbon linker chain to generate the neutral complex **1** (namely, **Re-1** for M = Re; **$^{99}$Tc-1** for M = $^{99}$Tc; and **$^{99m}$Tc-1** for M = $^{99m}$Tc) with the aim of developing a single-photon emission computed tomography (SPECT) radiodiagnostic agent for AD. **Re-1** was characterized by spectroscopic methods and X-ray crystallography, whereas the detailed NMR spectroscopic analysis of **$^{99}$Tc-1** demonstrated its structural similarity to **Re-1**. Complexes **Re-1** and **$^{99}$Tc-1** display selective binding affinity for amyloid plaques as evidenced by fluorescence spectroscopy, whereas the biodistribution data of **$^{99m}$Tc-1**—characterized by relatively low brain uptake, fast clearance from brain and blood, and in vivo stability—are considered encouraging for further elaboration on the structural features of **1** in the direction of increased brain uptake.

## Introduction

The development of specific positron emission tomography (PET) and/or single-photon emission computed tomography (SPECT) imaging agents for in vivo imaging of β-amyloid (Aβ) plaques of Alzheimer's disease (AD) represents an active area in radiopharmaceutical design.[1–3] Aβ plaques are one of the signature lesions of the AD brain that consist of fibrillar deposits of Aβ peptide,[4,5] and their in vivo visualization might therefore contribute to the definite and early diagnosis of AD. Furthermore, the spatially detailed information provided by radioimaging on the extent and propagation of pathology in the living brain could contribute to neuropathogenesis studies of AD and in the evaluation of the efficacy of antiamyloid therapies currently under investigation.[6]

Clinical trials in AD patients with several PET imaging agents labeled with either $^{11}$C or $^{18}$F resulted in imaging of Aβ plaques in living brain tissue[7–9] and demonstrated the potential utility of these agents. The most widely studied PET amyloid imaging agent is the 2-phenylbenzothiazole derivative 2-(4′-[$^{11}$C]methylaminophenyl)-6-hydroxybenzothiazole (Pittsburgh compound-B, [$^{11}$C]PiB), a neutral derivative of the amyloid binding dye thioflavin-T (Scheme 1) that is employed in clinical practice. The histological and

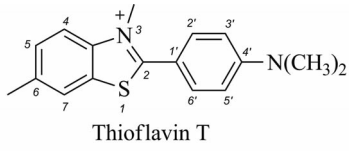


Thioflavin T

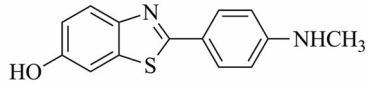


Pittsburg compound B (PiB)

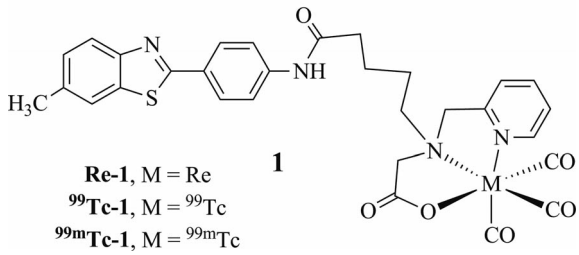


**Re-1**, M = Re
**$^{99}$Tc-1**, M = $^{99}$Tc
**$^{99m}$Tc-1**, M = $^{99m}$Tc

**1**

Scheme 1. Structures of thioflavin T, Pittsburg compound B (PiB), and complex **1**.

[a] Institute of Biology, National Centre for Scientific Research "Demokritos",
15310 Athens, Greece
Fax: +30-210-6511767
E-mail: pelmar@bio.demokritos.gr
Homepage: http://bio.demokritos.gr/index.php?option=com_content&view=article&id=39&Itemid=49&lang=en
[b] Institute of Materials Science, National Centre for Scientific Research "Demokritos",
15310 Athens, Greece
[c] Department of Inorganic Chemistry, University of Zürich, Winterthurerstrasse 191, 8053 Zürich, Switzerland
[d] Institute of Radioisotopes & Radiodiagnostic Products, National Centre for Scientific Research "Demokritos",
15310 Athens, Greece

Supporting information for this article is available on the WWW under http://dx.doi.org/10.1002/ejic.201200450.

  

biochemical specificity of PiB binding across different regions of the AD brain was demonstrated by the direct correlation of in vivo [$^{11}$C]PiB retention with region-matched quantitative analyses of Aβ plaques in the same subject.[2,8,10] However, due to the short half-life of $^{11}$C (20 min), the availability of [$^{11}$C]PiB is limited to on-site cyclotrons and sophisticated radiochemistry laboratories, and as a result, its structural analogue that contains the longer half-life (110 min) radioisotope $^{18}$F-fluorine has been introduced.[11] [$^{18}$F]3′-FPiB ($^{18}$F-Flutemetamol) performs similarly to [$^{11}$C]PiB, provides a wider accessibility for clinical and research use, and is currently in Phase III clinical trials.[12] The successful course of the PiB compound indicates that small-molecule amyloid imaging agents can be developed through structural modifications of thioflavin T.

Because PET scanners and the infrastructure for handling PET isotopes are only available to a limited number of modern hospitals, considerable effort has been directed toward the development of agents for imaging of Aβ plaques with SPECT, which is more widely used in routine diagnostic practice. Even though progress in developing imaging agents that target Aβ plaques is less advanced for SPECT than for PET, a variety of probes labeled with the SPECT isotopes $^{123}$I, $^{125}$I, or $^{99m}$Tc have been prepared and evaluated in in vitro and in vivo experiments.[13,14] In particular, the promising results obtained with PET-labeled PiB and the nearly optimal characteristics of technetium-99m as a radionuclide for nuclear imaging[15] have led to the synthesis of a number of complexes of $^{99m}$TcO(V)$^{3+}$, or of its congener ReO(V)$^{3+}$, with tetradentate $S_2N_2$ or $SN_3$ chelators carrying the 2-phenylbenzothiazole pharmacophore either through a linker[16–19] or integrated into the chelate moiety.[19] These $^{99m}$TcO(V)$^{3+}$ complexes showed affinity for Aβ plaques in vitro; however, their unfavorable in vivo pharmacokinetics in normal mice—characterized either by low brain uptake or by slow washout—has precluded their clinical testing,[13] thus suggesting that additional molecular modifications are required to improve their in vivo properties. Within the framework of the ongoing investigation of the development of a $^{99m}$Tc-based SPECT amyloid imaging agent, the synthesis of a new 2-phenylbenzothiazole complex with the M(CO)$_3^+$ tricarbonyl core (**1**; Scheme 1) with M = Re, $^{99}$Tc, and $^{99m}$Tc is herein reported along with its initial biological evaluation.

## Results and Discussion

### Design of Complex 1

In the design of complex **1**, 2-(4′-aminophenyl)-6-methylbenzothiazole (**2**, Scheme 2) was employed as the pharmacophore to render affinity for amyloid plaques. Compound **2** is a neutral derivative of thioflavin-T in which the methyl group on the heterocyclic nitrogen has been removed with consequent elimination of the positive charge from the benzothiazole ring. This removal is known to produce phenylbenzothiazole derivatives with increased lipophilicity and enhanced affinity for amyloid in vitro and in vivo.[8,20,21] In the final ligand **4** (which will be used in the form of its ethyl ester **4′**), compound **2** is joined through a pentanoyl linker to the metal-chelating moiety. The affinity and specificity of both **2** and **4′** for amyloid plaques was confirmed through in vitro staining experiments on brain tissue (Figure S1 in the Supporting Information). The purpose of the five-carbon linker chain is to alleviate the steric hindrance imposed by the bulkiness of the metal core and to allow interaction of the phenylbenzothiazole pharmacophore with amyloid plaques. It should be mentioned that in the case of the corresponding complex that bears a two-carbon linker chain,[22] no binding to the amyloid plaques was observed, a fact attributed to steric effects that are imposed by the bulkiness of the metal core.

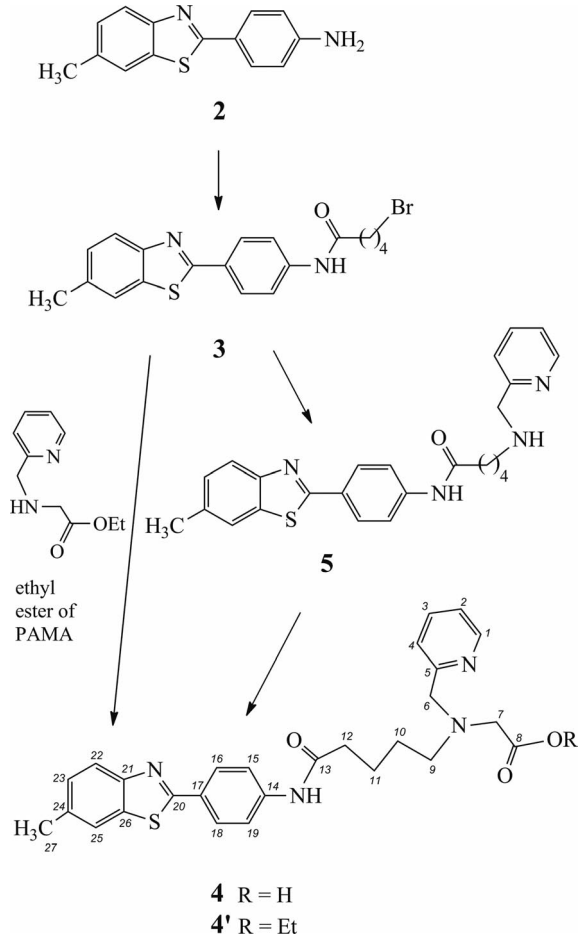


Scheme 2. Synthetic pathways leading to ligand **4**. The atom numbering is the one used for the NMR spectroscopic assignments presented in Table 1.

The organometallic *fac*-[$^{99m}$Tc(I)(CO)$_3$]$^+$ core was selected as an alternative to the $^{99m}$TcO(V)$^{3+}$ core employed so far in the literature for labeling of amyloid plaques because it forms kinetically stable complexes with high specific radioactivity and it is readily available through the Isolink® kit in a routine radiopharmaceutical environment.[23] Even though the $^{99m}$Tc-tricarbonyl agents as a class are not characterized by efficient crossing of the blood/brain bar-

  

rier, a number of complexes in the literature with tridentate[24–26] or bidentate[27] ligands have shown adequate crossing to justify the utilization of the $^{99m}$Tc-tricarbonyl core in the development of potential amyloid plaque imaging agents. The tridentate NNO ligand[15] picolylamine monoacetic acid (PAMA; Scheme 2) was selected as the chelator for the $^{99m}Tc(CO)_3^+$ core because it leads to stable, neutral complexes that display in vivo stability.[28–30] As is the usual practice in technetium radiochemistry,[31] the stable Re analogue was synthesized first for characterization and in vitro evaluation purposes. Chemistry was subsequently transferred at the pseudostable $^{99}$Tc and at the metastable $^{99m}$Tc level.

### Synthetic Procedure for Re-1 and $^{99}$Tc-1

For the synthesis of ligand **4′** (Scheme 2), the published procedure[32,33] involves acylation of the aromatic amine of **2** by 5-bromopentanoyl chloride to generate the bromide **3**, followed by nucleophilic attack of the nitrogen of the secondary amine of the ethyl ester of PAMA to generate ligand **4′** in the form of its ethyl ester **4′**. This synthetic scheme led to a fairly impure product that required repetitive flash chromatography separations for its purification (yield < 20%). To improve the procedure, a stepwise synthetic approach was employed in which the *N*-pentanoylbromide **3** initially reacted with 2-(methylamino)pyridine to yield **5** and subsequently, without purification, ethyl bromoacetate was used to attack the secondary amine formed. This approach led to the isolation of pure **4′** after a single flash chromatography column and at a significantly increased reaction yield (51% overall). A ligand-exchange reaction between **4′** and the organometallic $(NEt_4)_2[ReBr_3(CO)_3]$ precursor[21] in the presence of sodium hydroxide generated complex **Re-1** in high yield. Complex **Re-1** was crystallized from $CH_3OH$/water and was fully characterized by elemental analysis, spectroscopic techniques, and X-ray crystallography.

Complex **$^{99}$Tc-1** was synthesized in a similar way to its Re analogue by treating $(NEt_4)_2[^{99}TcCl_3(CO)_3]$ with ligand **4′** in MeOH.

The infrared spectra of complexes **Re-1** and **$^{99}$Tc-1** show strong bands at 2016, 1910, 1871, and at 2035, 1931, and 1915 $cm^{-1}$, respectively, which are attributed to stretching vibrations of the tricarbonyl *fac*-$[M(CO)_3]^+$ unit. In addition, the complexes exhibit strong broad absorptions in the 1600–1650 $cm^{-1}$ region that correspond to asymmetrical C=O stretching vibrations of the amide and the coordinated carboxylate groups.

The assignments of the $^1$H and $^{13}$C chemical shifts for ligand **4′** and complexes **Re-1** and **$^{99}$Tc-1** proceeded as described in detail for related *N*-derivatized PAMA complexes with the tricarbonyl *fac*-$[Re(CO)_3]^+$ core[28,29] and are presented in Table 1. NMR spectroscopic data for the corresponding free acid ligand **4** are given in Table S1 of the Supporting Information. Relative to ligand **4**, the spectra of **Re-1** and **$^{99}$Tc-1** display distinct features that indicate the coordination of ligand **4** around the metal core, namely: 1)

Table 1. $^1$H and $^{13}$C chemical shifts [ppm] for ligand **4′** and complexes **Re-1** and **$^{99}$Tc-1** in $[D_6]$DMSO at 25 °C. The numbering of the atoms is shown in Scheme 2.

| | **4′** | **Re-1** | **$^{99}$Tc-1** | | **4′** | **Re-1** | **$^{99}$Tc-1** |
|---|---|---|---|---|---|---|---|
| H-1 | 8.46 | 8.76 | 8.69 | C-1 | 148.64 | 151.97 | 151.80 |
| H-2 | 7.23 | 7.57 | 7.56 | C-2 | 122.10 | 125.84 | 125.21 |
| H-3 | 7.75 | 8.14 | 8.06 | C-3 | 136.44 | 140.52 | 140.09 |
| H-4 | 7.48 | 7.71 | 7.65 | C-4 | 122.53 | 123.91 | 123.68 |
| H-6 | 3.84 | 4.77/4.53 | 4.53/4.45 | C-5 | 159.47 | 159.61 | 158.86 |
| H-7 | 3.39 | 3.82/3.41 | 3.72/3.20 | C-6 | 59.71 | 67.37 | 66.55 |
| H-9 | 2.62 | 3.57/3.49 | 3.44 | C-7 | 54.44 | 60.81 | 61.61 |
| H-10 | 1.46 | 1.83/1.77 | 1.77 | C-8 | 170.84 | 178.81 | 177.01 |
| H-11 | 1.59 | 1.67 | 1.66 | C-9 | 53.19 | 69.12 | 68.15 |
| H-12 | 2.32 | 2.45 | 2.44 | C-10 | 26.66 | 23.99 | 23.70 |
| H-15/H-19 | 7.77 | 7.80 | 7.80 | C-11 | 22.66 | 22.17 | 21.98 |
| H-16/H-18 | 8.00 | 8.01 | 8.01 | C-12 | 36.24 | 35.99 | 35.72 |
| H-22 | 7.89 | 7.90 | 7.89 | C-13 | 171.64 | 171.34 | 171.09 |
| H-23 | 7.34 | 7.34 | 7.34 | C-14 | 141.96 | 141.94 | 141.97 |
| H-25 | 7.90 | 7.91 | 7.90 | C-15/C-19 | 119.16 | 119.31 | 119.26 |
| H-27 | 2.45 | 2.45 | 2.45 | C-16/C-18 | 127.78 | 127.85 | 127.85 |
| NH | 10.16 | 10.27 | 10.27 | C-17 | 127.43 | 127.57 | 127.55 |
| Et | 4.07, 1.17 | | | C-20 | 165.88 | 165.93 | 165.93 |
| | | | | C-21 | 151.77 | 151.80 | 151.90 |
| | | | | C-22 | 122.04 | 122.16 | 122.15 |
| | | | | C-23 | 127.98 | 128.05 | 128.05 |
| | | | | C-24 | 134.96 | 135.04 | 135.04 |
| | | | | C-25 | 121.75 | 121.80 | 121.80 |
| | | | | C-26 | 134.38 | 134.43 | 134.43 |
| | | | | C-27 | 21.02 | 21.07 | 21.07 |
| | | | | Et | 59.61, 14.11 | | |
| | | | | C≡O | | 197.24 | not |
| | | | | | | 197.76 | detectable |
| | | | | | | 197.87 | |

  

downfield shifts of the H-1 to H-4 protons of the pyridine moiety by $\delta$ = 0.2–0.6 ppm and of the corresponding C-1 to C-4 carbon atoms by $\delta$ = 1.3–4.6 ppm, 2) downfield shifts up to $\delta$ = 16 ppm of the C-6, C-7, C-8, and C-9 carbon atoms that are directly attached to the coordinating NNO atoms, 3) chemical-shift differentiation of the geminal protons on C-6, C-7, and C-9 that appear as doublet peaks with average downfield shifts of $\delta$ = 0.6–1 ppm (see Figure S2 in the Supporting Information). The chemical shifts of the protons and carbon atoms of the phenylbenzothiazole moiety that are distant from the metal do not show any appreciable changes upon coordination.

Comparison of the $^{1}$H chemical shifts between the **Re-1** and **$^{99}$Tc-1** complexes show a small metal dependence for the protons close to the coordination sphere, with Re resonances being more deshielded and $\Delta\delta_H$(Re,$^{99}$Tc) ranging from 0.01 to 0.2 ppm. With the exception of C-7, carbon atoms follow the same trend with $\Delta\delta_C$(Re,$^{99}$Tc) ranging from 0.2 to 1.8 ppm. Chemical-shift differentiation of the geminal protons on C-6 and C-7 is smaller for **$^{99}$Tc-1** than for **Re-1** and it becomes nonexistent for protons on C-9 and C-10 of the linker chain, thereby possibly indicating higher chelate mobility for the **$^{99}$Tc-1** complex than for **Re-1**. The **Re-1**/**$^{99}$Tc-1** comparison data are in agreement with the trends reported for $ReO(V)^{3+}$ and $TcO(V)^{3+}$ homologous complexes with diaminedithiols.[34]

## X-ray Crystallography of Re-1

Compound **Re-1** crystallizes in the triclinic space group $P\bar{1}$. The asymmetric unit contains one neutral rhenium complex and is partially occupied by water and methanol solvate molecules. The molecular structure of **Re-1** is given in Figure 1, and selected bond lengths and angles are listed in Table 2. The coordination geometry about rhenium is distorted octahedral and consists of the *fac*-$[Re(CO)_3]^+$ moiety and the NNO donor atom set of the tridentate ligand. The NNO donor atom set consists of a pyridine nitrogen, a tertiary amine nitrogen, and a carboxylato oxygen atom. The apical positions of the octahedron are occupied by the carboxylato oxygen of the tridentate ligand and one of the carbonyl groups. Rhenium lies almost in the equatorial plane defined by the two remaining carbonyl groups and the two coordinated nitrogen atoms of the tridentate ligand (displacement 0.09 Å). There are two five-membered rings in the coordination sphere (i.e., Re–N–C–C–N and Re–O–C–C–N). The former adopts the envelope configuration with C8 being 0.59 Å out of the best mean plane of the remaining four atoms. The latter is planar with the largest deviation from the mean plane being ca. 0.1 Å for C10. The Re–N2 bond length is slightly longer than the Re–N1, as expected on account of the $sp^3$ character of the former with respect to the $sp^2$-hybridization of the latter. The Re–C2 bond length is slightly shorter than the other two Re–CO bond lengths on account of the *trans* effect in the apical position. In the crystal lattice, the rhenium complexes form dimers on account of the strong hydrogen bonding between the amide NH group and the coordinated carboxylato oxygen atom of a neighboring complex [N3···O4 2.916 Å (1 – *x*, 1 – *y*, –*z*), H3N···O4 2.050 Å, N3–H3N···O4 168.3°].

Table 2. Selected bond lengths [Å] and angles [°] for **Re-1**.

| Bond lengths | | | |
|---|---|---|---|
| Re–C1 | 1.910(9) | Re–N1 | 2.183(6) |
| Re–C2 | 1.888(9) | Re–N2 | 2.227(5) |
| Re–C3 | 1.928(7) | Re–O4 | 2.125(5) |
| **Angles** | | | |
| C2–Re–C1 | 87.9(3) | C3–Re–N1 | 97.8(2) |
| C2–Re–C3 | 90.1(3) | O4–Re–N1 | 81.2(2) |
| C1–Re–C3 | 87.9(3) | C2–Re–N2 | 96.5(2) |
| C2–Re–O4 | 174.9(2) | C1–Re–N2 | 97.0(2) |
| C1–Re–O4 | 94.8(3) | C3–Re–N2 | 172.0(2) |
| C3–Re–O4 | 94.3(2) | O4–Re–N2 | 79.0(2) |
| C2–Re–N1 | 95.7(3) | N1–Re–N2 | 76.9(2) |
| C1–Re–N1 | 173.2(2) | | |

## Affinity of Re-1 and $^{99}$Tc-1 for Amyloid Plaques

The binding affinity of **Re-1** for Aβ plaques was tested with in vitro staining experiments with human AD brain tissue and observation under a fluorescence microscope. The phenylbenzothiazole moiety is fluorescent,[35] and complex **Re-1** retains the fluorescent properties with an absorbance maximum at 329 nm and an emission maximum at 378 nm (Figure S3 in the Supporting Information). Figure 2 shows microscope images of the stained brain tissue in which it is clear that complex **Re-1** clearly labels plaques with blue fluorescence. The results of staining of adjacent plaques with the histological dye thioflavin S, which is clinically used for the detection of amyloid plaques (Figure 2, B, D), demonstrate that **Re-1** labels plaques in a similar way

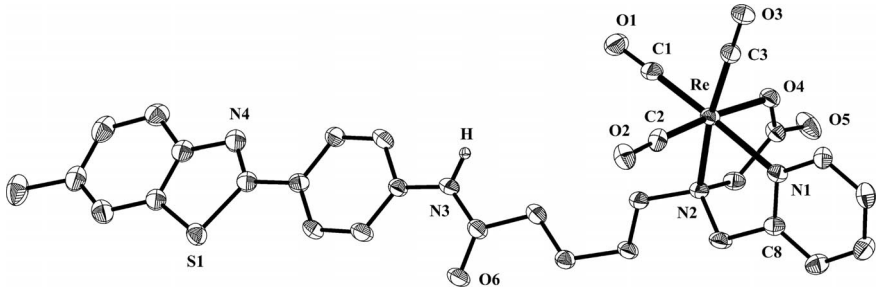


Figure 1. Partially labeled plot of **Re-1** with ellipsoids drawn at the 30% probability level. Hydrogen atoms (except that on N3) are omitted for clarity.

  

to thioflavin S. Similarly, complex **$^{99}$Tc-1** showed also the ability of in vitro labeling amyloid plaques (Figure S4 in the Supporting Information). These staining results, in combination with the lack of staining when a shorter acetamide linker was employed,[22] confirmed the hypothesis that in this type of complexes the phenylbenzothiazole pharmacophore has to be distanced from the metal core to interact with amyloid plaques.

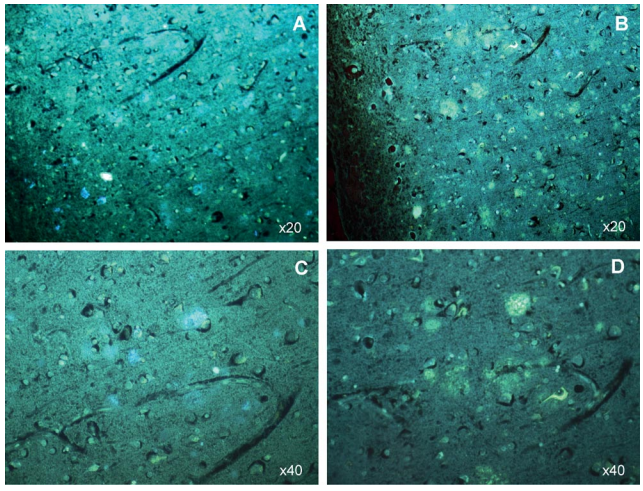


Figure 2. Fluorescence microscopy images of slices of Alzheimer's-diseased brain stained with (A, C) complex **Re-1** and (B, D) thioflavin S. The magnification of the lens is indicated on each picture. Slices A/B, C/D are adjacent to allow for comparison of the staining pattern between complex **Re-1** (blue fluoresence, max at 378 nm) and thioflavin S (yellow-green fluoresence, max at 550 nm). It is clear from the photos that complex **Re-1** stains amyloid plaques in a similar way to thioflavin S.

## Synthesis and Characterization of $^{99m}$Tc-1

Complex **$^{99m}$Tc-1** was prepared by a ligand-exchange reaction that employed the *fac*-$[^{99m}Tc(CO)_3(H_2O)_3]^+$ precursor as described previously[32,33] in a radiochemical yield of >95%. The identity of complex **$^{99m}$Tc-1** was established by comparative HPLC analysis using samples of the well-characterized complexes **Re-1** and **$^{99}$Tc-1** (Figure 3). The **$^{99m}$Tc-1** complex was stable in its preparation reaction mixture for a period of at least 6 h at room temperature and was also found stable against the histidine and cysteine challenge for the same period of time.

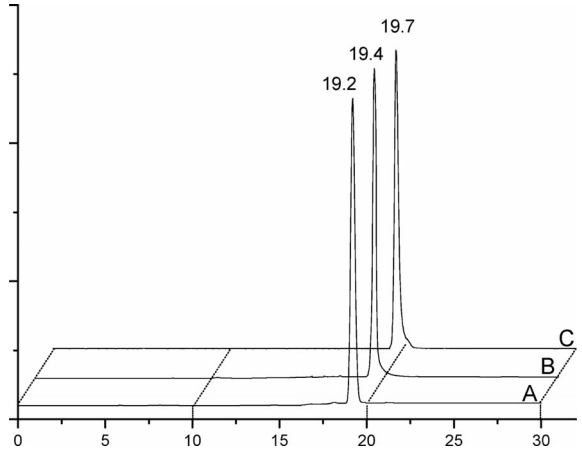


Figure 3. Comparative reverse-phase HPLC chromatograms. UV detection at 254 nm: (A) complex Re-1 and (B) complex $^{99}$Tc-1. Radiometric detection: (C) complex $^{99m}$Tc-1.

The lipophilicity of the **$^{99m}$Tc-1** complex was evaluated according to a literature procedure[36] by the determination of its partition coefficient ($P$) in *n*-octanol/0.1 M phosphate buffer (pH 7.4), which resulted in a $\log P_{oct/buffer}$ value of 1.69. This $\log P_{oct/buffer}$ value falls within the range of 1–2.5 considered ideal for potential brain-imaging agents.[37]

## Biodistribution of $^{99m}$Tc-1

Biodistribution studies of **$^{99m}$Tc-1** were carried out in healthy Swiss albino mice, and the results at 1, 15, and 60 min p.i. are presented in Table 4. The radioactivity measured in the brain tissue at 1 min is 0.69% ID/g (percentage of injected dose of radioactivity per gram of tissue), and at 15 min it is washed out, quickly dropping to 0.05% ID/g. The radioactivity rapidly clears from the blood and reaches 0.65 and 0.24% ID/g at 15 and 60 min, respectively. The low stomach and spleen values are indicative of the lack of in vivo oxidation of technetium to pertechnetate or Tc colloid. Excretion of radioactivity occurred mainly through the hepatobiliary system.

The biodistribution data for **$^{99m}$Tc-1** compare favorably to those that exist in the literature for related complexes with the phenylbenzothiazole moiety. Specifically, a potential $^{99m}$TcO–monoamine–monoamide ($^{99m}$TcO–MAMA) tracer conjugated to pheynylbenzothiazole through a five-carbon alkoxy chain,[18] despite its high initial brain uptake (1.34% ID/g at 2 min p.i.), is associated with high blood background (4.43% ID/g at 60 min), which is unfavorable for imaging applications. Other potential $^{99m}$TcO–bis-amine-bis-thiol ($^{99m}$TcO–BAT) complexes conjugated to phenylbenzothiazole through either alkoxy[16] or amide[17] linker chains show low brain uptake between 0.1 and 0.2% ID/organ at 2 min accompanied by low in vivo stability and the generation of pertechnetate and hydrophilic metabolites that result in high levels of radioactivity in the blood (5.7–8.8% ID/organ at 60 min) and in the stomach (4.7–5.8% ID/organ at 60 min) that preclude their further investigation. Complex **$^{99m}$Tc-1** lacks the negative characteristics (high blood background, reoxidation to pertechnetate) of the other potential phenylbenzothiazole tracers in the literature, and even though its % ID brain uptake in normal mice is relatively low, this percentage might increase in pathological AD mice in which binding to amyloid plaques and retention of radioactivity is anticipated. Overall, the biodistribution results justify the further improvement of the structural characteristics of **$^{99m}$Tc-1** with an aim towards increased brain uptake. Overall, the biodistribution results justify the further improvement of the structural characteristics of **$^{99m}$Tc-1** (e.g., by replacing the pentanoyl by a butyl linker chain, or replacing the amide functionality of the linker with amine) according to increased brain uptake.[37,38]

  

## Conclusion

Complex **1**, in which the tricarbonyl [M(CO)$_3$NNO] chelate is joined to the 2-(4′-aminophenyl)-6-methylbenzothiazole according to the pendant approach, was successfully synthesized and fully characterized at the macroscopic (**Re-1** and **$^{99}$Tc-1**) and the non-carrier-added technetium (**$^{99m}$Tc-1**) level. To the best of our knowledge, the X-ray crystallographic structure of complex **Re-1** is the first example of a complex with a pendant phenylbenzothiazole pharmacophore to be presented in the literature. The NMR spectroscopic study of **Re-1** and **$^{99}$Tc-1** clearly demonstrates their anticipated structural similarity and provides comparative Re/Tc data of use in spectral assignments of similar [M(CO)$_3$NNO] (M = Re, $^{99}$Tc) complexes.

Both **Re-1** and **$^{99}$Tc-1** selectively label amyloid plaques in vitro with blue fluorescence, thus demonstrating that the binding affinity of the 2-(4′-aminophenyl)-6-methylbenzothiazole pharmacophore is maintained in the complexes. These results further demonstrate that analogous Re/Tc complexes interact with amyloid plaques in a similar way, thereby expanding the range of similar Re/Tc properties described in the literature.

The **$^{99m}$Tc-1** radioactive analogue displays in vitro stability and ideal lipophilicity for brain uptake. Its biodistribution data in healthy mice – characterized by relatively low initial brain uptake, fast clearance from the brain and the blood, and lack of in vivo re-oxidation – are overall judged as positive and prompt for further elaboration on this $^{99m}$Tc–tricarbonyl NNO system, as bearing potential to generate agents for imaging of amyloid plaques.

## Experimental Section

**Materials and Methods:** Reagents and solvents were purchased from Aldrich Chemical Co or Fluka Chemical Co and used without further purification. Na$^{99m}$TcO$_4$ was obtained in physiological saline as commercial $^{99}$Mo/$^{99m}$Tc generator eluate (Cis International). Flash column chromatography was performed with Merck silica gel 60. C, H, and N analysis was performed with a Perkin–Elmer 2400 automatic elemental analyzer. High-performance liquid chromatography (HPLC) analysis was performed with a Waters 600E Chromatography System coupled to both a Waters 991 photodiode array detector (UV trace for Re and $^{99}$Tc complexes) and a GABI gamma detector from Raytest ($\gamma$ trace for $^{99m}$Tc complexes). Solvents used in chromatographic analysis were HPLC grade. Separations were achieved with a Macherey–Nagel Nucleosil C18 (10 μ, 250 × 4.6 mm) column eluted with a binary gradient system at a 1.0 mL min$^{-1}$ flow rate. Mobile phase A was 0.1% trifluoroacetic acid (TFA) in methanol, whereas mobile phase B was 0.1% TFA in water. The elution profile was: 0 to 1 min 0% of phase A followed by a linear gradient to 75% of phase A in 9 min; this composition was held for another 20 min. After a column wash with 95% of phase A for 5 min, the column was re-equilibrated by applying the initial conditions (0% of phase A) for 15 min prior to the next injection. IR spectra were recorded in the range 4000–500 cm$^{-1}$ with a Perkin–Elmer 1600 FTIR spectrophotometer as KBr pellets and with a Nicolet 6700 ATR-IR from Thermo Scientific. NMR spectra were acquired at 25 °C in [D$_6$]-DMSO with a 500 MHz Bruker DRX-Avance spectrometer ($^1$H at 500.13 MHz and $^{13}$C at 125.77 MHz). Assignment of $^1$H and $^{13}$C NMR spectroscopic chemical shifts was based on two-dimensional $^1$H,$^1$H and $^1$H,$^{13}$C correlation experiments (COSY, NOESY, HSQC, HMBC) were recorded using standard pulse sequences. The chemical shifts for $^1$H and $^{13}$C are reported in ppm ($\delta$) relative to tetramethylsilane (TMS).

The starting pharamcophore 2-(4′-aminophenyl)-6-methylbenzothiazole (**2**) as well as the precursors (NEt$_4$)$_2$[ReBr$_3$(CO)$_3$], (NEt$_4$)$_2$-[$^{99}$TcCl$_3$(CO)$_3$] and *fac*-[$^{99m}$Tc(CO)$_3$(H$_2$O)$_3$]$^+$ were prepared according to published procedures.[21,33,39]

**5-Bromo-*N*-[4-(6-methylbenzothiazol-2-yl)phenyl]pentanamide (3):** 5-Bromopentanoyl bromide (1.37 g, 6.86 mmol) was added dropwise and under nitrogen to a stirred solution of **2** (1.5 g, 6.14 mmol), and triethylamine (0.95 g, 9.25 mmol) in dry $CH_2Cl_2$ (10 mL) at 0 °C. The reaction mixture was stirred for 30 min at 0 °C and then for 2.5 h at room temperature under nitrogen. The precipitate that was formed during the reaction was filtered, washed with cold dichloromethane, and air-dried to afford product **3** as pale yellow powder that was purified by flash chromatography (1% methanol/chloroform); yield 83%. $^1$H NMR (500 MHz, [D$_6$]-DMSO): $\delta$ = 10.23, 8.01, 7.90, 7.89, 7.78, 7.34, 7.23, 3.57, 2.54, 2.40, 1.87, 1.74; 171.2, 165.8, 151.7, 141.8, 134.9, 134.3, 127.9, 127.7, 127.4, 122.0, 121.7, 119.1, 60.9, 35.3, 34.7, 31.6, 23.5, 20.9 ppm. $C_{19}H_{19}BrN_2OS$ (403.34): calcd. C 56.58, H 4.75, N 6.95; found C 56.80, H 4.78, N 6.92.

***N*-[4-(6-Methylbenzothiazol-2-yl)phenyl]-5-[(pyridin-2-ylmethyl)-amino]pentanamide (5):** A solution of the bromide **3** (2.5 g, 6.2 mmol) in toluene (30 mL) was treated with a fivefold excess amount of 2-(aminomethyl)pyridine (3.35 g, 31 mmol) under reflux conditions overnight. The reaction mixture was filtered while hot and, upon cooling, the resulting precipitate was washed with ice-cold 1% $Na_2CO_3$. The product was used without further purification; yield 75%. $^1$H NMR (500 MHz, [D$_6$]DMSO): $\delta$ = 10.25, 8.62, 8.01, 7.90, 7.89, 7.88, 7.87, 7.85, 7.78, 7.51, 7.4, 7.34, 7.39, 4.32, 4.19, 3.00, 2.45, 2.42, 1.66; 179.8, 169.0, 161.3, 151.4, 148.6, 139.6, 138.5, 135.7, 134.1, 129.0, 126.6, 121.3, 124.1, 121.5, 120.9, 119.7, 52.5, 48.8, 38.0, 29.5, 23.0, 20.8 ppm.

**Ethyl *N*-[4-(Benzothiazol-2-yl)phenylaminocarbonylbutyl]-*N*-(pyridin-2-ylmethyl)aminoacetate (4′):** Ethyl bromoacetate (1.4 g, 9 mmol) was added to a stirred solution of **5** (1.25 g, 3 mmol) and triethylamine (1.13 g, 12 mmol) in dry THF (40 mL) under nitrogen. The reaction mixture was heated at reflux for 16 h. It was then cooled to room temperature, filtered, and the solvent was evaporated to dryness. The residue was purified by means of flash column chromatography (hexane/ethyl acetate, 7:3 to 5:5) to afford the pure product as an off-white solid; yield 68%. $^1$H and $^{13}$C NMR spectroscopic chemical shifts are given in Table 1. $C_{29}H_{32}N_4O_3S$ (516.66): calcd. C 67.42, H 6.24, N 10.84; found C 67.24, H 6.32, N 10.97.

**Complex Re-1:** A mixture of ligand **4′** (100 mg, 0.2 mmol), the precursor [NEt$_4$]$_2$[ReBr$_3$(CO)$_3$] (154 mg, 0.2 mmol) in acetonitrile (5 mL), and NaOH (2 mL, 0.1 N, 0.2 mmol) was heated to reflux for 4 h. Upon standing at room temperature a pale yellowish crystalline product precipitated and was collected by filtration; yield 75%. $t_R$: 19.2 min. IR: $\tilde{\nu}$ = 2016, 1909, 1868, 1651 cm$^{-1}$. Crystals suitable for X-ray analysis were isolated by slow evaporation from a mixture of methanol/water. $^1$H and $^{13}$C NMR spectroscopic chemical shifts are given in Table 1. $C_{30}H_{27}N_4O_6ReS$ (757.83): calcd. C 47.55, H 3.59, N 7.39; found C 47.74, H 3.62, N 7.42.

**Complex $^{99}$Tc-1:** A mixture of ligand **4′** (41 mg, 0.08 mmol) and (NEt$_4$)$_2$[$^{99}$TcCl$_3$(CO)$_3$] (25 mg, 0.05 mmol) in MeOH (6 mL) was heated to reflux for 8 h. Upon standing at room temperature, a

  

pale yellowish crystalline product precipitated and was collected by filtration; yield 86%. $t_R$: 19.4 min. IR: $\tilde{\nu}$ = 2035, 1931, 1915, 1649 $cm^{-1}$. $^1H$ and $^{13}C$ NMR spectroscopic chemical shifts are given in Table 1.

**X-ray Structure Determination of Re-1:** A crystal with approximate dimensions 0.12 × 0.14 × 0.45 mm was taken from the mother liquor and immediately cooled to –93 °C. Diffraction measurements were made with a Rigaku R-AXIS SPIDER Image Plate diffractometer using graphite-monochromated Cu-$K_\alpha$ radiation. Data collection ($\omega$-scans) and processing (cell refinement, data reduction, and empirical absorption correction) were performed with the CrystalClear program package.[40] The structure was solved by direct methods using SHELXS-97 and refined by full-matrix least-squares techniques on $F^2$ with SHELXL-97.[41] Important crystallographic data are listed in Table 3. Further experimental crystallographic details for **Re-1**: $2\theta_{max}$ = 130°; reflections collected/unique/used, 20390/5002 ($R_{int}$ = 0.0548)/5002; 468 parameters refined; $(\Delta/\sigma)_{max}$ = 0.004; $(\Delta\rho)_{max}/(\Delta\rho)_{min}$ = 1.441/–1.126 e Å$^{-3}$; $R_1/wR_2$ (for all data), 0.0488/0.1180. Hydrogen atoms were located by difference maps and were refined isotropically or were introduced at calculated positions as riding on bonded atoms. All non-hydrogen atoms were refined anisotropically, except for the water and methanol solvate molecules, which were refined isotropically with occupation factors fixed to 0.4 and 0.3, respectively.

Table 3. Summary of crystal, intensity collection, and refinement data for **Re-1**.

| | **Re-1**·0.4$H_2O$·0.3$CH_3OH$ |
|---|---|
| Empirical formula | $C_{30.3}H_{31}N_4O_{6.7}ReS$ |
| $M_r$ | 776.65 |
| $T$ [°C] | –93 |
| $\lambda$ (Cu-$K_\alpha$) | 1.54178 |
| Space group | $P\bar{1}$ |
| $a$ [Å] | 11.3996(2) |
| $b$ [Å] | 11.7390(2) |
| $c$ [Å] | 12.7464(2) |
| $\alpha$ [°] | 80.435(1) |
| $\beta$ [°] | 67.914(1) |
| $\gamma$ [°] | 86.331(1) |
| $V$ [Å$^3$] | 1558.58(5) |
| $Z$ | 2 |
| $D_{calcd.}$ [Mg m$^{-3}$] | 1.655 |
| $\mu$ [mm$^{-1}$] | 8.680 |
| $F$(000) | 771 |
| Goodness-of-fit on $F^2$ | 1.068 |
| $R$ indices | $R1$ = 0.0440[a], $wR2$ = 0.1121[a] |

[a] For 4494 reflections with $I > 2\sigma(I)$.

CCDC-875335 contains the supplementary crystallographic data for this paper. These data can be obtained free of charge from The Cambridge Crystallographic Data Centre via www.ccdc.cam.ac.uk/data_request/cif.

**In vitro Binding of Re-1 and $^{99}$Tc-1 to Amyloid Plaques:** Postmortem brain tissue from an autopsy-confirmed AD case was obtained through the University of Manchester of the Greater Manchester Neurosciences Centre. Serial sections (6 μm thick) of paraffin-embedded blocks from temporal cortex mounted on albumin-coated glass slides were used for staining. Tissue sections were deparaffinized with two 5 min washes in xylene, two 3 min washes in 100% ethanol, 5 min washes in 80% ethanol/$H_2O$, 5 min washes in 60% ethanol/$H_2O$, running tap water for 10 min, and then incubated in phosphate buffer solution (PBS; 1.3 M NaCl, 27 mM KCl, 81 mM $Na_2HPO_4$, 14.7 mM $KH_2PO_4$, pH 7) for 30 min. The tissue preparations were treated with **Re-1** and **$^{99}$Tc-1** solutions in [$D_6$]DMSO (approximately 1 mg mL$^{-1}$) for 1 h. The sections were finally washed with 40% ethanol for 2 min, followed by rinsing with tap water for 30 s. Fluorescent observation was performed with a Zeiss Axioplan2 microscope (lens magnification as specified in each image) equipped with DAPI filter set.

**Synthesis of $^{99m}$Tc-1:** A freshly prepared solution (400 μL) of the *fac*-[$^{99m}$Tc(CO)$_3$($H_2O$)$_3$]$^+$ precursor (pH 7) was added to a vial that contained a solution of **4** (50 μg) in acetonitrile (100 μL). The vial was sealed, flushed with $N_2$, and heated for 20 min at 70 °C. HPLC analysis demonstrated the formation of a single complex ($t_R$ = 19.7 min, radiochemical yield >95%) that was stable for at least 6 h. The radioactivity recovery of the HPLC column was monitored and found to be quantitative. The identity of complex **$^{99m}$Tc-1** was established by comparative HPLC using samples of the well-characterized complexes **Re-1** and **$^{99}$Tc-1** (Figure 3).

**Determination of Partition Coefficient of $^{99m}$Tc-1:** The partition coefficient of **$^{99m}$Tc-1** was determined by the shake-flask method.[36] The HPLC-purified $^{99m}$Tc complex (10 μL) was mixed with 1-octanol (1.5 mL) and phosphate buffer (1.5 mL, 0.1 M, pH 7.4) in a centrifuge tube. The mixture was vortexed at room temperature for 1 min and finally centrifuged at 5000 rpm for 5 min. Three samples (0.2 mL each) were drawn both from the octanol and the aqueous layer and counted in a $\gamma$ counter. The experiment was run in triplicate. The partition coefficient ($\log P_{oct/buffer}$) was calculated by dividing the cpm/mL$_{(oct)}$ to cpm/mL$_{(buffer)}$, and the $\log P_{oct/buffer}$ was found to be 1.69.

**Stability of $^{99m}$Tc-1 against Cysteine and Histidine:** Aliquots of **$^{99m}$Tc-1** (70 μL) were added to a 1 mM cysteine or a 1 mM histidine solution (630 μL) in PBS, pH 7.4. The samples were incubated at 37 °C and analyzed by HPLC after 1, 3, and 6 h. Complex **$^{99m}$Tc-1** remained unaffected by the presence of cysteine or histidine.

**Biodistribution Studies of $^{99m}$Tc-1:** All the biodistribution studies were carried out in compliance with the national laws related to

Table 4. Biodistribution results of **$^{99m}$Tc-1** in healthy mice ($n$ = 5).

| | % ID/g | | | | | | % ID/organ | | | | | |
|---|---|---|---|---|---|---|---|---|---|---|---|---|
| | 1 min | | 15 min | | 60 min | | 1 min | | 15 min | | 60 min | |
| | AVG | STD | AVG | STD | AVG | STD | AVG | STD | AVG | STD | AVG | STD |
| Blood | 15.03 | 2.49 | 0.65 | 0.09 | 0.24 | 0.08 | 27.23 | 3.87 | 1.27 | 0.14 | 0.48 | 0.11 |
| Liver | 15.61 | 0.37 | 29.36 | 3.27 | 15.52 | 1.62 | 26.58 | 3.48 | 43.82 | 1.02 | 25.35 | 6.22 |
| Heart | 9.20 | 1.89 | 1.56 | 0.22 | 0.65 | 0.25 | 0.91 | 0.07 | 0.18 | 0.02 | 0.08 | 0.03 |
| Kidney | 11.48 | 1.09 | 12.30 | 3.15 | 3.56 | 0.68 | 3.44 | 0.27 | 4.17 | 0.71 | 1.27 | 0.17 |
| Stomach | 1.32 | 0.29 | 0.92 | 0.46 | 0.87 | 0.16 | 0.44 | 0.04 | 0.40 | 0.10 | 0.32 | 0.11 |
| Intestine | 1.34 | 0.27 | 10.91 | 1.92 | 17.54 | 2.98 | 3.98 | 0.64 | 28.98 | 2.69 | 43.92 | 4.66 |
| Spleen | 2.07 | 0.10 | 0.60 | 0.11 | 0.35 | 0.14 | 1.02 | 0.11 | 0.17 | 0.03 | 0.08 | 0.02 |
| Muscle | 1.56 | 0.22 | 0.49 | 0.05 | 0.24 | 0.04 | 17.31 | 1.59 | 5.92 | 0.32 | 2.94 | 0.24 |
| Lungs | 15.19 | 2.57 | 2.90 | 0.47 | 1.30 | 0.26 | 3.11 | 0.42 | 0.65 | 0.07 | 0.27 | 0.03 |
| Brain | 0.69 | 0.08 | 0.05 | 0.01 | 0.02 | 0.01 | 0.28 | 0.03 | 0.02 | 0.00 | 0.01 | 0.00 |

  

the conduct of animal experimentation. HPLC-purified $^{99m}$**Tc-1** (1–2 μCi in 0.1 mL methanol/saline 10:90) was injected through the tail vein in three groups of five Swiss Albino mice each [male, (26 ± 3) g]. The animals were sacrificed by cardiectomy under slight ether anaesthesia at predetermined time intervals (1, 15, and 60 min). The organs of interest were excised, weighed, and the radioactivity counted in an automatic $\gamma$ counter. The stomach and intestines were not emptied of food contents prior to radioactivity measurements. The percentage of injected dose per organ (% ID/organ) was calculated by comparison of sample radioactivity to standard solutions that contained 10% of the injected dose. The percentage of injected dose per gram (% ID/g) was calculated by dividing the % ID/organ by the weight of the organ or tissue. The calculation for blood and muscle were based upon measured activity, sample weight, and body composition data, considering that blood comprises 7% and muscle 43% of body weight. The biodistribution data are presented in Table 4.

**Supporting Information** (see footnote on the first page of this article): Fluorescence microscope images showing the staining of amyloid plaques by pharmacophore **2** and ligand **4**; $^1$H NMR spectra of ligand **4**, **Re-1**, and $^{99}$**Tc-1**; $^1$H and $^{13}$C NMR spectroscopic data of ligand **4**; UV absorbance and fluorescence spectra of complex **Re-1**; and fluorescence microscope images from consecutive AD brain slides stained with complex $^{99}$**Tc-1** and thioflavin S.

## Acknowledgments

The authors thankfully acknowledge financial support on this project by the John S. Latsis Public Benefit Foundation as well as the generous support of Professor David Mann of the Greater Manchester Neurosciences Centre, University of Manchester, in the AD brain-tissue staining experiments. They also thank Dr. K. Stamatakis of the Institute of Biology of NCSR "Demokritos" for obtaining the fluorescence spectra in his laboratory.

[1] K. Nagren, C. Halldin, J. O. Rinne, *Eur. J. Nucl. Medicine Mol. Imaging* **2010**, *37*, 1575–1593.
[2] M. Ewers, R. A. Sperling, W. E. Klunk, M. W. Weiner, H. Hampel, *Trends Neurosci.* **2011**, *34*, 430–442.
[3] C. A. Mathis, Y. Wang, W. E. Klunk, *Curr. Pharm. Des.* **2004**, *10*, 1469–1492.
[4] H. W. Querfurth, F. M. LaFerla, *New England J. Medicine* **2010**, *362*, 329–344.
[5] J. Hardy, D. J. Selkoe, *Science* **2002**, *297*, 353–356.
[6] N. Okamura, S. Furumoto, H. Arai, R. Iwata, K. Yanai, Y. Kudo, *Curr. Medical Imaging Rev.* **2008**, *4*, 56–62.
[7] H. Quigley, S. J. Colloby, J. T. O'Brien, *Int. J. Geriatric Psychiatry* **2011**, *26*, 991–999.
[8] S. Vallabhajosula, *Seminars Nucl. Medicine.* **2011**, *41*, 283–299.
[9] A. Nordberg, *Lancet Neurol.* **2004**, *3*, 519–527.
[10] W. E. Klunk, H. Engler, A. Nordberg, Y. Wang, G. Blomqvist, D. P. Holt, M. Bergstrom, I. Savitcheva, G. F. Huang, S. Estrada, B. Ausen, M. L. Debnath, J. Barletta, J. C. Price, J. Sandell, B. J. Lopresti, A. Wall, P. Koivisto, G. Antoni, C. A. Mathis, B. Langstrom, *Ann. Neurol.* **2004**, *55*, 306–319.
[11] R. Vandenberghe, K. Van Laere, A. Ivanoiu, E. Salmon, C. Bastin, E. Triau, S. Hasselbalch, I. Law, A. Andersen, A. Korner, L. Minthon, G. Garraux, N. Nelissen, G. Bormans, C. Buckley, R. Owenius, L. Thurfjell, G. Farrar, D. J. Brooks, *Ann. Neurol.* **2010**, *68*, 319–329.
[12] S. Vallabhajosula, L. Solnes, B. Vallabhajosula, *Seminars Nucl. Medicine* **2011**, *41*, 246–264.
[13] M. Ono, H. Saji, *Int. J. Mol. Imaging* **2011**, *2011*, 543267.
[14] Y. Cheng, M. Ono, H. Kimura, M. Ueda, H. Saji, *J. Med. Chem.* **2012**, *55*, 2279–2286.
[15] S. S. Jurisson, J. D. Lydon, *Chem. Rev.* **1999**, *99*, 2205–2218.
[16] K. Serdons, D. Vanderghinste, M. Van Eeckhoudt, J. Cleynhens, T. de Groot, G. Bormans, A. Verbruggen, *J. Labelled Compd. Radiopharm.* **2009**, *52*, 227–235.
[17] K. Serdons, T. Verduyckt, J. Cleynhens, C. Terwinghe, L. Mortelmans, G. Bormans, A. Verbruggen, *Bioorg. Med. Chem. Lett.* **2007**, *17*, 6086–6090.
[18] X. J. Chen, P. R. Yu, L. F. Zhang, B. Liu, *Bioorg. Med. Chem. Lett.* **2008**, *18*, 1442–1445.
[19] K. S. Lin, M. L. Debnath, C. A. Mathis, W. E. Klunk, *Bioorg. Med. Chem. Lett.* **2009**, *19*, 2258–2262.
[20] W. E. Klunk, Y. Wang, G. F. Huang, M. L. Debnath, D. P. Holt, C. A. Mathis, *Life Sci.* **2001**, *69*, 1471–1484.
[21] R. Alberto, A. Egli, U. Abram, K. Hegetschweiler, V. Gramlich, P. A. Schubiger, *J. Chem. Soc., Dalton Trans.* **1994**, 2815–2820.
[22] S. Tzanopoulou, G. Patsis, M. Sagnou, I. Pirmettis, M. Papadopoulos, M. Pelecanou, in: *Technetium, Rhenium and Other Metals in Chemistry and Nuclear Medicine*, vol. 7 (Ed.: U. Mazzi), SG Editoriali, Padova, Italy, **2006**, pp. 103–104.
[23] R. Alberto, *Med. Organometallic. Chem.* **2010**, *32*, 219–246.
[24] D. Rattat, J. Cleynhens, C. Terwinghe, A. E. De Greve, A. Verbruggen, *Tetrahedron Lett.* **2006**, *47*, 4641–4645.
[25] R. Garcia, L. Gano, L. Maria, A. Paulo, I. Santos, H. Spies, *J. Biol. Inorg. Chem.* **2006**, *11*, 769–782.
[26] D. Satpati, K. Bapat, A. Mukherjee, S. Banerjee, K. Kothari, M. Venkatesh, *Appl. Radiat. Isot.* **2006**, *64*, 888–892.
[27] J. B. Zhang, X. B. Wang, C. Jin, *J. Radioanal. Nucl. Chem.* **2007**, *272*, 91–94.
[28] P. Kyprianidou, C. Tsoukalas, A. Chiotellis, D. Papagiannopoulou, C. P. Raptopoulou, A. Terzis, M. Pelecanou, M. Papadopoulos, I. Pirmettis, *Inorg. Chim. Acta* **2011**, *370*, 236–242.
[29] A. Chiotellis, C. Tsoukalas, M. Pelecanou, C. Raptopoulou, A. Terzis, M. Papadopoulos, Z. Papadopoulou-Daifoti, I. Pirmettis, *Eur. J. Inorg. Chem.* **2008**, *47*, 2601–2607.
[30] R. La Bella, E. Garcia-Garayoa, M. Langer, P. Blauenstein, A. G. Beck-Sickinger, P. A. Schubiger, *Nucl. Med. Biol.* **2002**, *29*, 553–560.
[31] E. Deutsch, K. Libson, J. L. Vanderheyden, A. R. Ketring, H. R. Maxon, *Nucl. Med. Biol.* **1986**, *13*, 465–477.
[32] S. Tzanopoulou, I. C. Pirmettis, G. Patsis, M. Paravatou-Petsotas, E. Livaniou, M. Papadopoulos, M. Pelecanou, *J. Med. Chem.* **2006**, *49*, 5408–5410.
[33] S. Tzanopoulou, M. Sagnou, M. Paravatou-Petsotas, E. Gourni, G. Loudos, S. Xanthopoulos, D. Lafkas, H. Kiaris, A. Varvarigou, I. C. Pirmettis, M. Papadopoulos, M. Pelecanou, *J. Med. Chem.* **2010**, *53*, 4633–4641.
[34] M. Pelecanou, K. Chryssou, C. I. Stassinopoulou, *J. Inorg. Biochem.* **2000**, *79*, 347–351.
[35] J. Dey, S. K. Dogra, *J. Phys. Chem.* **1994**, *98*, 3638–3644.
[36] H. Yamauchi, J. Takahashi, S. Seri, H. Kawashima, H. Koike, M. Kato-Azuma, in: *Technetium and Rhenium in Chemistry and Nuclear Medicine 3* (Eds.: M. Nicolini, M. Bandoli, U. Mazzi), Cortina International, Verona, Italy, **1989**, pp. 475–502.
[37] D. D. Dischino, M. J. Welch, M. R. Kilbourn, M. E. Raichle, *J. Nucl. Med.* **1983**, *24*, 1030–1038.
[38] H. Pajouhesh, G. R. Lenz, *NeuroRx* **2005**, *2*, 541–553.
[39] R. Alberto, R. Schibli, A. Egli, A. P. Schubiger, U. Abram, T. A. Kaden, *J. Am. Chem. Soc.* **1998**, *120*, 7987–7988.
[40] *Rigaku/MSC*, Rigaku/MSC Inc., The Woodlands, Texas, USA, **2005**.
[41] G. M. Sheldrick, University of Göttingen, Germany, **1997**.

Received: May 3, 2012
Published Online: ■

  

EurJIC European Journal of Inorganic Chemistry

**Imaging Agents**

The *fac*-[M(NNO)$(CO)_3$] complex (M = Re, $^{99}$Tc, and $^{99m}$Tc) conjugated to 6-methyl-2-(4′-aminophenyl)benzothiazole was synthesized, completely characterized, and biologically evaluated in vitro and in vivo as a potential amyloid imaging agent.

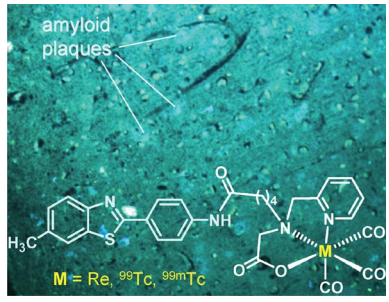




**Keywords:** Medicinal chemistry / Imaging agents / Rhenium / Technetium / Alzheimer's disease

  